Journal of Cleaner Production 296 (2021) 126520

Contents lists available at ScienceDirect

Journal of Cleaner Production

journal homepage: www.elsevier.com/locate/jclepro

Detection of rainwater harvesting ponds by matching terrain attributes with hydrologic response

Juan D. Márquez [a], Luis E. Peña [b, *], Miguel Barrios [c], Julián Leal [c]

[a] Research Group GMAE, Universidad de Ibagué, Ibagué, Carrera 22 Calle 67 B/Ambalá, 730001, Ibagué, Colombia
[b] Civil Engineering Program, Faculty of Engineering, Universidad de Ibagué, Carrera 22 Calle 67 B/Ambalá, 730001, Ibagué, Colombia
[c] Department of Engineering, Faculty of Forest Engineering, Universidad Del Tolima, Barrio Santa Helena Parte Alta, Ibagué, 730006299, Ibagué, Colombia

ARTICLE INFO

Article history:
Received 19 August 2020
Received in revised form
10 February 2021
Accepted 22 February 2021
Available online 25 February 2021

Handling editor; Zhifu Mi

Keywords:
Rainwater harvesting ponds
Pond detection
Terrain curvature analysis
Principal component analysis

ABSTRACT

Rainwater harvesting has proven to be a valuable strategy for mitigating the effects of global climate change. However, most of the techniques reported in the academic literature are based on capturing surface runoff generated by rainfall, and therefore, ponds are located close to surface currents, implying investments in infrastructure to conduct water to the place where it is utilized. The aims of this research are the following: i) develop a methodology for the detection of ponds for rainwater harvesting through hydrological and geospatial analyses based on terrain curvature, and ii) identify relevant variables to establish the potential storage volume in ponds. For this purpose, the study was performed in the Tolima region of Colombia with an area of 23,663 km^2, where 32% corresponds to arid and semi-arid areas. The detection of ponds from the terrain curvature was carried out using geographic information systems and the estimation of daily storage in the rainwater harvesting pond (RWHP) system. Likewise, the principal component analysis identified key variables in the process of detecting and selecting ponds. The results show that the proposed methodology allows the detection of potential ponds for rainwater harvesting near cultivation and water demanding zones for various uses, which could introduce relevant variables in decision-making processes and, decrease water supply distribution costs in semi-arid areas.

1. Introduction

Water-supply related problems are found worldwide, limiting the development of economic activities (Sayl et al., 2016). Likewise, the constant population growth and the consequent expansion of agricultural areas increase water demand (Wambura et al., 2018). Simultaneously, studies have estimated that climate change is influencing the intensity and frequency of droughts, and reducing water availability in some regions (Li et al., 2018), being more severe in arid and semi-arid areas, especially in developing countries (Adham et al., 2019). The growing need for water access leads to the search for alternative supply sources that can be used for agriculture and human consumption (Kumar and Jhariya, 2017). In this sense, water collection and storage in rainwater harvesting (RWH) systems has been a successful strategy to mitigate the effects of climate change (Wu et al., 2018), and expand areas with perennial crops (Rosell et al., 2017).

The effectiveness of rainwater systems is related to the identification or detection of areas suitable for this practice (Ammar et al., 2016). *Detection* criteria are based on the evaluation of hydrogeomorphological characteristics that facilitate the capture, transport, and storage of rainwater together with socio-economic aspects that enhance their use benefit (Wu et al., 2018). Various methodologies to identify appropriate areas for RWH have been developed in recent decades, among which algorithms based on geographic information systems (GIS) (e.g., Singhai et al., 2019; Tiwari et al., 2018; Kadam et al., 2012), GIS-based multi-criteria analyses (e.g., Grum et al., 2016; Singh et al., 2017), and hierarchical analytical processes based on GIS, stand out (e.g., Balkhair and Ur Rahman, 2019; Shadeed et al., 2019). Hence, in all cases, modeling has been limited to the elaboration of suitability maps for RWH at the basin scale, without considering specific site characteristics or particular project drawbacks. This is decisive for selecting the system in terms of efficiency and low implementation cost (Terêncio et al., 2017).

In this context, the systems proposed in the literature are

* Corresponding author.
E-mail addresses: 2520131028@estudiantesunibague.edu.co (J.D. Márquez), luis.pena@unibague.edu.co (L.E. Peña), mibarrios@ut.edu.co (M. Barrios), jlealv@ut.edu.co (J. Leal).

https://doi.org/10.1016/j.jclepro.2021.126520

focused on the collection of surface runoff generated by rains in suitable basins to carry out RWH. Consequently, to collect the highest amount of surface runoff, some authors have included thematic analyzes of potential runoff (Singhai et al., 2019; Kumar et al., 2016), and in the drainage network, accumulated flow cells from a digital elevation model (DEM) have been used (Kumar and Jhariya, 2017; Mbilinyi et al., 2007). The previous is carried out to locate the storage structures at the watershed outlet on the surface currents, thus, calculating potential volumes of accumulated water on the drainage network (Shadmehri Toosi et al., 2020). This practice contributes positively to the efficient use of available natural resources and the reduction in erosion, floods, and vulnerability to the occurrence of droughts (Kanta et al., 2017). However, decreases in the average river flow have also been reported, leading to negative hydrological, socio-economic, and environmental impacts for users located downstream (Ngigi et al., 2007). Furthermore, increases in evapotranspiration reduce percolation, especially in dry years (Wambura et al., 2018), and increases in water consumption in the upper parts of streams limit water availability to sustain downstream ecosystem services (Welderufael et al., 2013). Conversely, Adham et al. (2018) evaluated the sustainability of ponds considering criteria such as slope, soil texture, vegetation cover, surface runoff, and the order of the main channel, as most of the methodologies locate ponds in areas adjacent to streams. Likewise, a tool that calculates the variables considered in the maps to evaluate the sustainability of a pond was employed.

It is worth mentioning that only a few studies have reported detection techniques for potential storage in places far from water currents. This could improve the water availability, and spatial distribution of water for agricultural and human consumption uses in remote areas, reducing conduction or distribution costs (Shadeed et al., 2019).

This study introduces a methodological process for detecting rainwater harvesting ponds (RWHP) based on the physical analysis of the terrain curvature profile by applying geographic information systems (GIS). So the detection focuses on using the land shape for storing rainwater in places away from surface currents. The estimation of water storage and identifying key variables in the selection process of detected ponds will be carried out by simulating the behavior of rain in the application area, corresponding to the arid and semi-arid zones of the Tolima region in Colombia. As part of the evaluation process, a principal component analysis (PCA) was performed to identify relationships between the potential water storage volume and variables, such as pond area, water storage in RWHP, and geomorphological attributes, including the slope and the catchment area of the pond.

2. Study area

The Tolima region is located in the center-west region of Colombia between coordinates 02° 52′ N to 05° 19′ N and 74° 24′ W to 76° 06′ W, with an area of 24,011 km^2 (Fig. 1). It includes elevation ranges between 199 and 5215 m a.s.l., with an average value of 1672 m a.s.l. The report of 98 meteorological stations shows a bimodal precipitation regime with an average annual precipitation of 1922 mm (monthly average value of 160 mm). October, November, and December are the months with the highest amount of rain, while June, July, August, and September are the driest months of the year. Likewise, the average temperature is 22.3 °C, the average annual evapotranspiration value is 1191 mm, and the monthly average is 99 mm.

According to Instituto Geográfico Agustín Coddazi (IGAC, 2004), the northern region of the study area includes deep sandy soils of volcanic origin, well-drained, and with medium textures; there are also superficial sandy soils of sandstone origin, excessively drained with medium and thick textures. In the east, very superficial soils of sandstone origin, excessively drained, with medium and thick textures; moderately deep alluvial sediment soils, moderately well-drained of varying textures are also found. To the south, superficial soils of clay-sandstone origin, excessively drained thick, and medium texture; there are also moderately deep soils of tonalite and granodiorite origins, well-drained, with medium to coarse textures. To the west, superficial soils of pyroclastic origin on andesites, well-drained and with thick textures; moreover, deep and superficial soils of volcanic ash origin on shales, well-drained with medium textures. According to the classification of the Natural Resources Conservation Service (NRCS, 2009), a representative portion of the study area is comprised of sandy textures and silty sand (Group A), covering an area of 11,196 km^2, i.e., approximately 47% of the study area. The following soil groups have silty clay (Group C) and clay (Group D) textures covering 6145 km^2 and 3794 km^2, respectively. According to the classification of the United States Department of Agriculture, the Tolima region has mostly a low potential to generate surface runoff, followed by some areas that have moderate to high potential for surface runoff. The land cover map was reclassified into four groups (Fig. 2d): grasses, crops, forests, and impervious surfaces; the latter includes urbanized areas, nature reserves, environmental protection areas, and glacial zones.

3. Materials and methods

3.1. Information collection and pre-processing

The information used for this study comes mainly from government organizations, and in this case, a soil texture map from the Colombian geographic institute [Instituto Geográfico "Agustín Codazzi"] (IGAC, 2004), a land cover map of the Autonomous Regional Environmental Corporation of Tolima [Corporación Autónoma Regional del Tolima] (CORTOLIMA), and a digital elevation model of the National Aeronautics and Space Administration (NASA) of the United States Federal Government. The coordinate system adopted for cartographic information corresponds to Magna Colombia Bogotá 3116.

Precipitation and daily temperature series from 98 meteorological stations in an average period of 30 years (1987–2017) were obtained from the Institute of Hydrological, Meteorological and Environmental Studies (Instituto de Hidrología, Meteorología y Estudios Ambientales [IDEAM]). Daily evapotranspiration values were calculated with the modified Turc method (Turc, 1961). Average monthly precipitation and evapotranspiration data were interpolated using the inverse distance weighted (IDW) method in ArcGis, appropriate for Colombia (González-Álvarez et al., 2019). Based on soil information units, a soil reclassification was made to obtain the map of hydrological groups, according to NRCS (2009). Likewise, the soil vegetation cover was reclassified into four groups: grass, crops, forests, and impervious surfaces. Finally, two digital elevation models (DEM) with resolutions of 30.86 m and 12.50 m were used to develop the method.

3.2. Detection and selection of potential storage areas for rainwater harvesting ponds (RWHP)

The detection of rainwater harvest ponds (RWHP) was performed by intersecting thematic layers of non-convex surface profile curvatures, flow accumulation with their established threshold values, and grass-like soil cover data. The non-convex curvature of the surface allows taking advantage of the geoform to collect and store rainwater without making major interventions on the terrain. Flow accumulation, together with flow accumulation

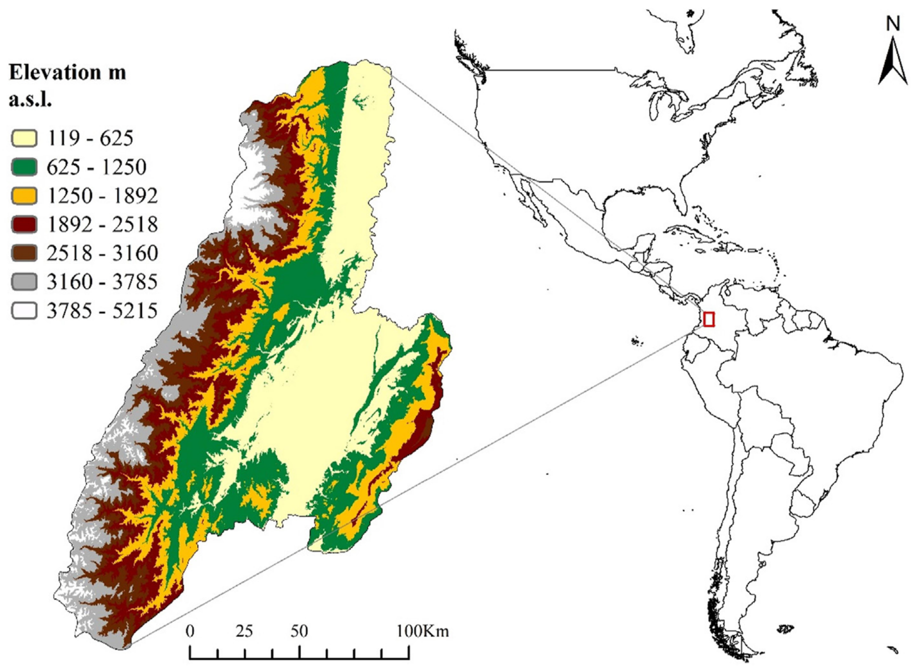

Fig. 1. Study area.

threshold values, allows extracting the current channels of the digital elevation model, and, thus, avoid placing the RWHP on them. Finally, the grass cover allows taking advantage of areas that do not compromise forested vegetation and existing crops, hence, causing a lower environmental impact for rainwater harvesting; additionally, rainwater harvesting structures are prevented from being viewed as a waste of productive land, as indicated by Kumar et al. (2016). Intersected cells or pixels obtain their respective elevation value from the DEM.

Following the detection procedure, a selection process for representative RWHP was carried out. RWHP detected with an area (A_p) larger than 9000 m^2 and change in storage (Δ_S) in November (average from 1987 to 2017) higher than or equal to 90 mm (Fig. 2f) were selected. The water storage criterion is similar to the one proposed by Mugo and Odera (2018) to determine suitable rainwater harvesting areas. Additionally, using the "Watershed" tool in ArcGIS, an afferent area (A_c) was outlined for each RWHP, in which the direct runoff generated there is collected and stored by the RWHP. A summary of the methodology is presented in Fig. 3.

3.2.1. Curvature

The ArcGis "curvature" tool was used to obtain the curvature of the terrain. This tool calculates the value, cell by cell, of the second derivative of the terrain surface, as proposed by Zevenbergen and Thorne (1987). The terrain profile curvature was exclusively analyzed due to its effects on flow acceleration, erosion, and sedimentation rate (Domazetović et al., 2019; Moore et al., 1991). The profile curvature is negative for convex cells, zero (0) for flat cells, and positive for concave cells (Akumu et al., 2019). Therefore, this study focused on non-convex cells, given their relationship with flow slow down, and low erosion (Dornik et al., 2018; MacMillan et al., 2000).

3.2.2. Flow accumulation

The flow accumulation value was obtained from the D8 algorithm since it has been widely used to delineate drainage networks from the DEM, incorporated in the ArcGIS "Flow accumulation" tool. However, it has limitations to define the correct flow accumulation threshold value to start the delineation (Ariza-Villaverde et al., 2013). Multiple studies of flow network extraction from digital elevation models (e.g., Gopinath et al., 2014; Persendt and Gomez, 2016) show that flow accumulation is the critical factor influencing the geomorphology of the network (Luo et al., 2008). In this sense, it was necessary to define a threshold value for the flow accumulation to extract the current channels. However, this value varies due to the influence of the DEM resolution and some attributes of the terrain (Ariza-Villaverde et al., 2015). Therefore, the flow accumulation threshold value used for the study area was 100 accumulated cells, considering the results obtained by various authors (Chen et al., 2016; Oyebande and Adeaga, 2006). Finally, four flow accumulation threshold values were chosen to perform RWHP detection; these values were 8, 16, 32, and 64 accumulated cells for DEMs of 30.86 m and 12.50 m.

3.3. Estimation of the stored volume in RWHP

The stored volume was calculated only for the RWHP resulting from the described selection process. As mentioned above, these are comprised of two parts: pond and afferent area; the pond is coated with plastic sheets or waterproofing geotextiles (Assefa et al., 2016), and the afferent area is an area attached to the pond covered with the site vegetation (catchment runoff). The components of an RWHP are shown in Figs. 2 and 4.

Concerning the above, it was necessary to calculate the direct runoff generated obtained by the method published by the Natural Resources Conservation Service (NRCS), previously known as SCS-CN (USDA-SCS, 1972), as shown in Eq. (1) and Eq. (2). This method has been widely used in rainwater harvesting research (e.g., Napoli et al., 2014; Tiwari et al., 2018).

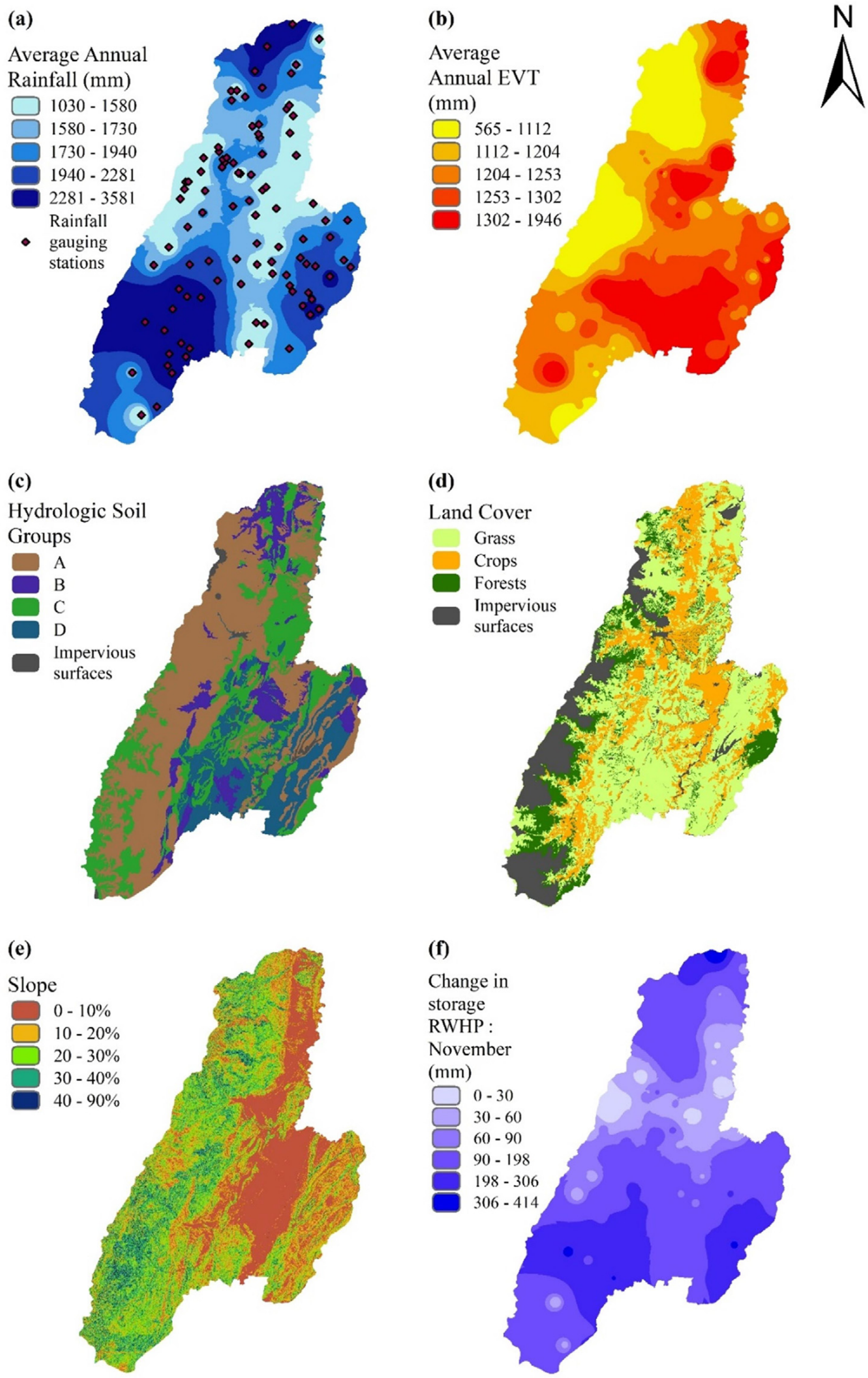

Fig. 2. a. Precipitation. b. Evapotranspiration. c. Soil texture per hydrological group. d. Reclassified vegetation cover. e. Slope. F. Change in storage at RWHP (Δ_S) during November.

$$Q(t) = \begin{cases} \dfrac{(P(t) - 0.2S)^2}{(P(t) + 0.8S)} \ if\ P(t) > 0.2S \\ 0 \quad otherwise \end{cases} \tag{1}$$

$$S = \frac{25400}{CN} - 254 \tag{2}$$

where $Q(t)$ is the direct runoff in mm on the t-th day, $P(t)$ is precipitation in mm on the t-th day, and S is the maximum potential retention in mm. The calculation of S is obtained from its transformation to the curve number (CN), given that the study area does not have infiltration values (Peña et al., 2016). In Colombia, the use

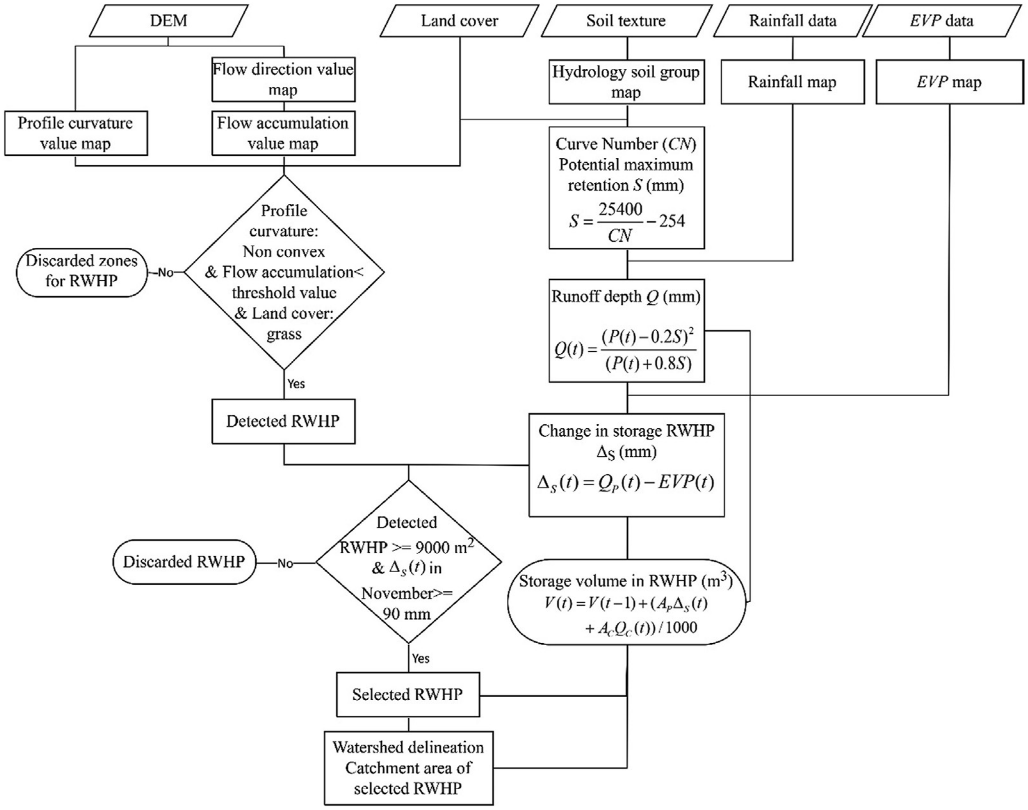

Fig. 3. Proposed process for the detection and selection of ponds for rainwater harvesting focused on the non-convex curvature of the surface.

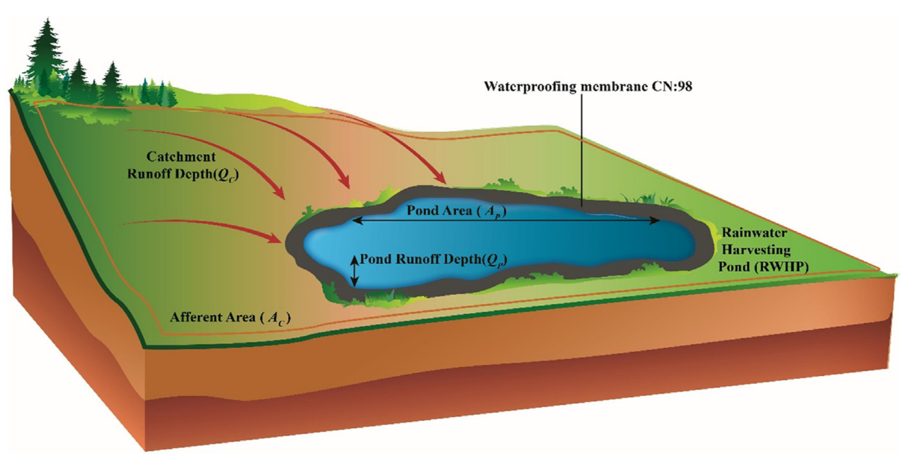

Fig. 4. Components of a selected rainwater harvesting pond (RWHP).

of *CN* values has been reported to describe the hydrological behavior in catchments in various soil use configurations (e.g., Santos- Jaimes et al., 2018; Uribe et al., 2018; Zabaleta et al., 2018). The *CN* values used for the different types of soil and vegetation cover were allocated (Table 1). In this sense, the direct pond runoff ($Q_P(t)$) was calculated with a *CN* of 98, corresponding to a waterproofing geotextile used in a pond, and direct runoff from the afferent area ($Q_C(t)$), with a *CN* corresponding to the soil type and vegetation cover of the site.

Considering that the water harvested by an RWHP is affected by solar radiation during the storage period, it was necessary to make an adjustment for evaporation losses in the RWHP. Eq. (3) represents the change in storage in the RWHP, where $\Delta_S(t)$ is the change in storage on the *t*-th day (mm), and *EVP*(*t*) is the evaporation in mm on the *t*-th day; however, for this study, potential

Table 1
Curvature number (*CN*) values employed in the study area.

Land cover	Hydrologic soil group			
	A	B	C	D
Grass	49	69	79	84
Crops	67	78	85	89
Forests	36	60	73	79
Impervious surface	98	98	98	98
Waterproofing geotextile in a pond	98	98	98	98

evapotranspiration ($EVT(t)$) was used.

$$\Delta_S(t) = Q_P(t) - EVP(t) \quad (3)$$

Finally, the volume stored in RWHP was obtained using Eq. (4), where $V(t)$ is the cumulative volume stored in RWHP (m^3) after the end of the t-th day, A_C is the afferent area (m^2), and A_P is the pond area (m^2). In this study, the maximum storage volume for each pond was defined by a depth of 2.0 m, and the pond area was defined by applying the detection algorithm of the terrain curvature available in geographic information systems (Fig. 4). In this way, the occurrence of possible overflows was considered, as stated by Imteaz et al. (2012).

$$V(t) = \begin{cases} V(t-1) + (A_P \Delta_S(t) + A_C Q_C(t))/1000 \\ 0 \quad \text{for } V(t) < 0 \\ 2A_P \quad \text{for } V(t) > 2A_P \end{cases} \quad (4)$$

3.4. Storage and discharge scenarios in RWHP

Three storage and discharge scenarios were proposed to analyze the water volume stored and its corresponding offer for each RWHP. These scenarios focus mainly on supplying water during dry periods (Table 2). The supply of RWHP depends on the water volume collected in the storage and discharge periods. To this end, the period from October 1992 up to September 1993 was selected as the mean hydrological year, according to the values of the Oceanic Niño Index (ONI) (National Weather Service, 2020). Therefore, the volume stored in a pond was estimated, considering runoff and daily storage (Eq. (5)), where $V_{Ei}(t)$ is the cumulative volume stored in RWHP (m^3) after the end of the t-th day in scenario Ei, and α is the water demand equivalent to 0.0% at the storage period, with 1.0%; 0.5%, or 0.1% of the volume available the day before in each pond at the discharge period.

$$V_{Ei}(t) = \begin{cases} V(t-1) - \alpha V(t-1) + (A_P \Delta_S(t) + A_C Q_C(t))/1000 \\ 0 \quad \text{for } V(t) < 0 \\ 2A_P \quad \text{for } V(t) > 2A_P \end{cases} \quad (5)$$

3.5. Principal component analysis

A principal component analysis (PCA) was performed to reduce the dimensionality of the data set with interrelated variables (Sharma and Tiwari, 2009). In this case, the following variables were analyzed: annual stored volume (Vp), RWHP area (A_p), afferent area of the RWHP (A_c), precipitation $_{(P)}$, potential evapotranspiration (EVT), average change in storage in the RWHP (Δ_S), terrain slope in the RHWP area (β), and elevation where the RWHP is located (E).

4. Results and discussion

The precipitation records in the 98 meteorological stations of the study area show an average annual precipitation range of 1030 to 3581 mm (Fig. 2a), where more than 60% is recorded in October, November, December, and afterward in March, April, and May. On the other hand, the annual average evapotranspiration registers an interval between 565 up to 1946 mm (Fig. 2b), and June, July, August, and September are the driest months. Therefore, rainwater collection and storage will be carried out mainly in the months with the highest precipitation. In contrast, discharge or emptying will occur in the months with the highest pressure on the water resource due to the decrease in rainfall.

4.1. RWHP detection and selection

The results obtained in the detection and selection of the RWHP for the different flow accumulation thresholds in the digital elevation models with a cell size of 30.86 m (DEM 30.86) and 12.50 m (DEM 12.50), are presented in an aggregate form in Table 3, and its spatial distribution is observed in Fig. 5. When the flow accumulation threshold value increases, there is an increase in the amount of RWHP detected and selected; likewise, the increase is higher by improving the DEM resolution.

With DEM 30.86, around 6.3 million RWHP were detected with areas between 953 m^2 and 152,423 m^2. Meanwhile, in DEM 12.50, approximately 29.9 million RWHPs with areas between 156 m^2 and 375,469 m^2 were identified. From the above, it is essential to point out that the difference between the amount of RWHP detected is because, in DEM 12.50, the RWHP observed has a smaller area compared to DEM 30.86; in the case of the minimum area, this difference is around 84%. Therefore, it is convenient to mention the total extension of the RWHP detected in the study area. Furthermore, 28% of the surface was identified as RWHP with DEM 30.86, and 26% with DEM 12.50. This result suggests that an increase in DEM resolution leads to an increase in the number of RWHP detected over a smaller area extension. These results are consistent with the study carried out by Ariza-Villaverde et al. (2015), where the strong influence of the digital elevation model resolution on the geomorphology of a surface was recorded.

For the RWHP selection process, a positive relationship is found between the number of RWHP selected, and the flow accumulation threshold value. For 64 accumulated cells, 1365 RWHP were selected in DEM 30.86, whose areas range between 9526 m^2 and 152,423 m^2. Likewise, for DEM 12.50, 9925 RWHP with areas between 9062 m^2 and 375,469 m^2 were selected. Based on the above, the increase in the selected RWHP was estimated in 8560 ponds, representing an increase of 627%. Unlike the detection results obtained, the extension values of the area occupied by the selected RWHP with DEM 12.50 exceed DEM 30.86 in 171 km^2 (0.71%). Therefore, to select RWHP, the increase in the DEM resolution leads to an increase in the number of RWHP selected, occupying a larger extension of the total study area.

Table 2
Storage and discharge scenarios.

Scenario ID	Description of rainwater harvested in a pond	Storage	Discharge
E1	Twelve storage and gradual emptying cycles in each of the 12 months of the year. Potential offer every month of the year.	Monthly	Monthly
E2	Two storage cycles in the two wet periods of the area and gradual emptying during the two dry periods. Potential offer six months per year.	Oct, Nov, Dec & Mar, Apr, May	Jan, Feb & Jun, Jul, Aug, Sep
E3	Single storage cycle in the eight most humid months and gradual emptying throughout the driest period. Potential offer four months per year.	Oct, Nov, Dec, Jan, Feb, Mar, Apr, May	Jun, Jul; Aug, Sep

Table 3
Rainwater harvesting ponds (RWHP) that meet the selection criteria defined in this study.

Flow accumulation threshold value	DEM 30							DEM 12.50						
	RWHP Detected			RWHP Selected				RWHP Detected			RWHP Selected			
	Quantity (millions)	Area (km^2)	Area (%)	Quantity	Area (km^2)	Area (%)	Average volume stored (m^3/RWHP)	Quantity (millions)	Area (km^2)	Area (%)	Quantity	Area (km^2)	Area (%)	Average volume stored (m^3/RWHP)
8	5.17	5382.92	22.42	506	6.05	0.03	20,001	21.90	4271.28	17.79	1476	21.12	0.09	23,929
16	5.72	6006.68	25.02	790	9.40	0.04	19,618	26.17	5275.02	21.97	5077	75.29	0.31	25,663
32	6.07	6418.16	26.73	1081	12.88	0.05	19,971	28.61	5902.81	24.58	8008	138.04	0.57	29,910
64	6.28	6684.52	27.84	1365	16.20	0.07	20,295	29.85	6252.70	26.04	9925	187.44	0.78	32,427

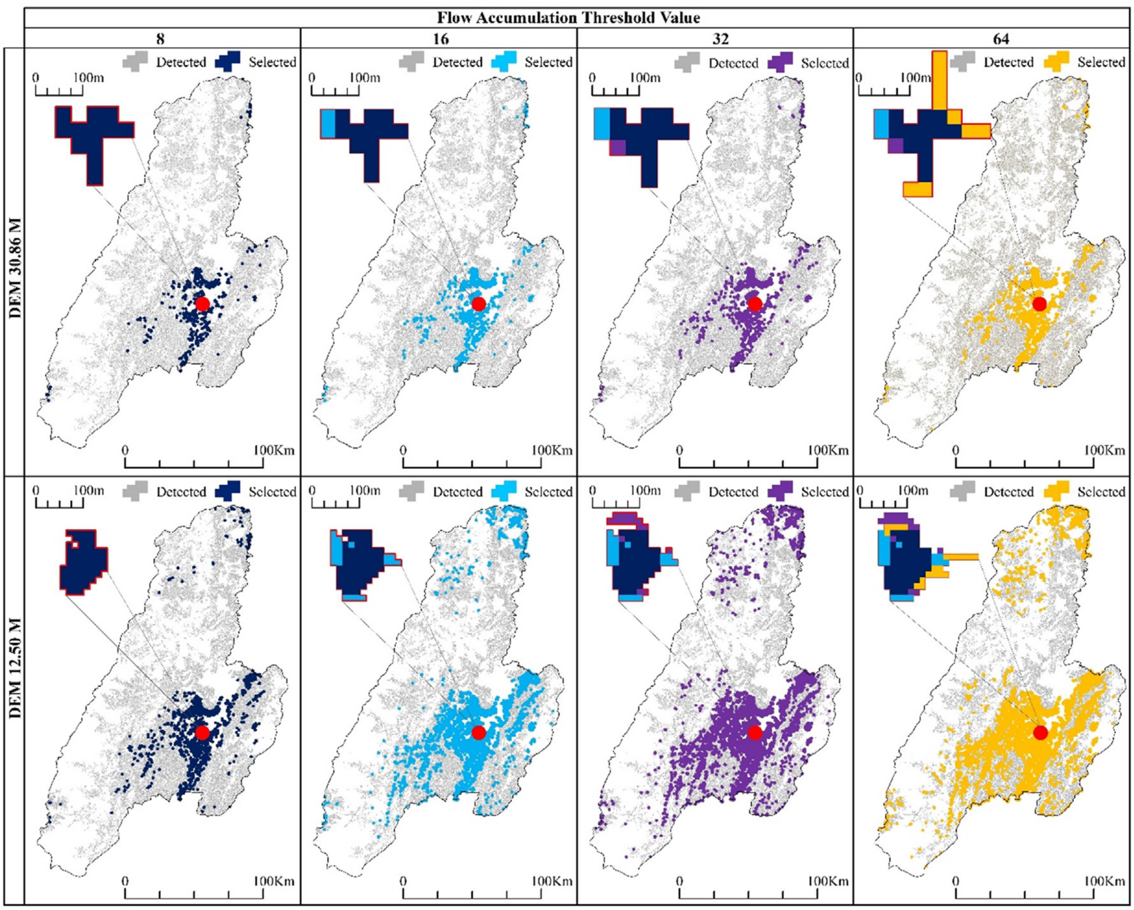

Fig. 5. Rainwater harvesting ponds (RWHP) detected and selected through the increase in the flow accumulation threshold value (8, 16, 32, and 64 accumulated cells).

On the other hand, the results show that for DEM 12.50 and 64 accumulated cells, 5585 out of 9925 selected RWHP were located in areas with slopes between 6% and 12%, representing 56% of the ponds. Similar results were found by Jamali and Ghorbani (2020) and Wu et al. (2018), where slopes of 5%–10% were considered highly suitable for identifying rainwater harvesting sites. Likewise, Mahmoud & Alazba (2015) found that slopes between 2% and 8% attained a higher degree of suitability, which is a consequence of the relationship between the slope and erosion processes.

Additionally, in the particular case of a pond selected for the different flow accumulation threshold values and DEM resolutions (Fig. 5), it is important to highlight that, for each flow accumulation threshold value, the pond changes its shape, generally increasing its area. This, in turn, allows the RWHP to improve its rainwater storage capacity. Likewise, when comparing the selected ponds among the DEMs used, differences in size and shape are identified. Based on the results obtained in this study, DEM 12.50 and 64 accumulated cells were the appropriate parameters to achieve the highest number of RWHP selected.

4.2. Volume stored in the RWHP

From the selected RWHP, the annual average storage that each pond will have was estimated (Fig. 6). It is important to note that for a given area value, there are multiple volumes, and, likewise, an increase in the RWHP area usually means an increase in the volume collected and stored. This is because by increasing the storage capacity of the RWHP, overflow losses decrease. Likewise, a positive and linear correlation is observed between the stored volume and the RWHP area. (Fig. 6); therefore, an increase in storage area could be related to a larger volume stored. Conversely, it is possible to identify the minimum volume stored as a function of the area

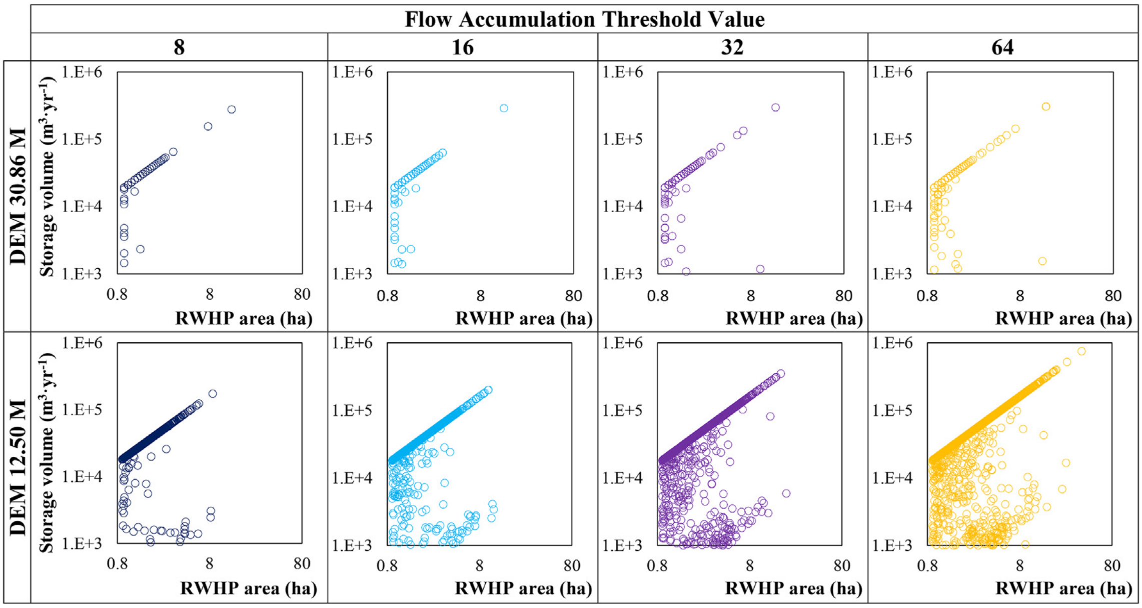

Fig. 6. Rainwater volume stored concerning the area of the selected pond, per flow accumulation threshold value, and digital elevation model (DEM).

afferent to the RWHP, which is higher when detecting with the 12.5 m DEM compared to the 30.8 m DEM (Fig. 7). Similar results were found by Jung et al. (2014). Additionally, DEM 12.50 and a flow accumulation threshold value of 64 accumulated cells were the most representative values in terms of selected RWHP and stored volume for the study area.

The RWHP selected from DEM 12.50, and the flow accumulation threshold value were chosen to evaluate the storage and discharge scenarios previously described in the methodology (Fig. 8).

In the first scenario (E1), the supply available for each pond is carried out on a monthly basis throughout the year, and the influence of the precipitation regime is notable. In October, December, and May, the highest storages are recorded, while in June, July and August, the storages are close to 0.0 m^3. The average volume that can be offered by each of the ponds in E1 corresponds to the following values: 7.69 $m^3 \cdot day^{-1}$ for a water demand of 0.1% of the available volume; 27.50 $m^3 \cdot day^{-1}$ for a water demand of 0.5%; and 38.38 $m^3 \cdot day^{-1}$ for a water demand of 1.0%.

In scenario E2, the available supply is carried out in two discharge cycles in the two dry periods of the bimodal precipitation regime, corresponding to a first discharge in January and February, followed by a second discharge in June, July, August, and September. By contrasting the results obtained in E1, scenario E2 defines a more extended storage period, contributing to increasing the volume available for discharge. The average volume offered by each of the ponds in this scenario corresponds to the following values: 8.00 $m^3 \cdot day^{-1}$ for a water demand of 0.1% of the available volume; 31.73 $m^3 \cdot day^{-1}$ for a water demand of 0.5%; and

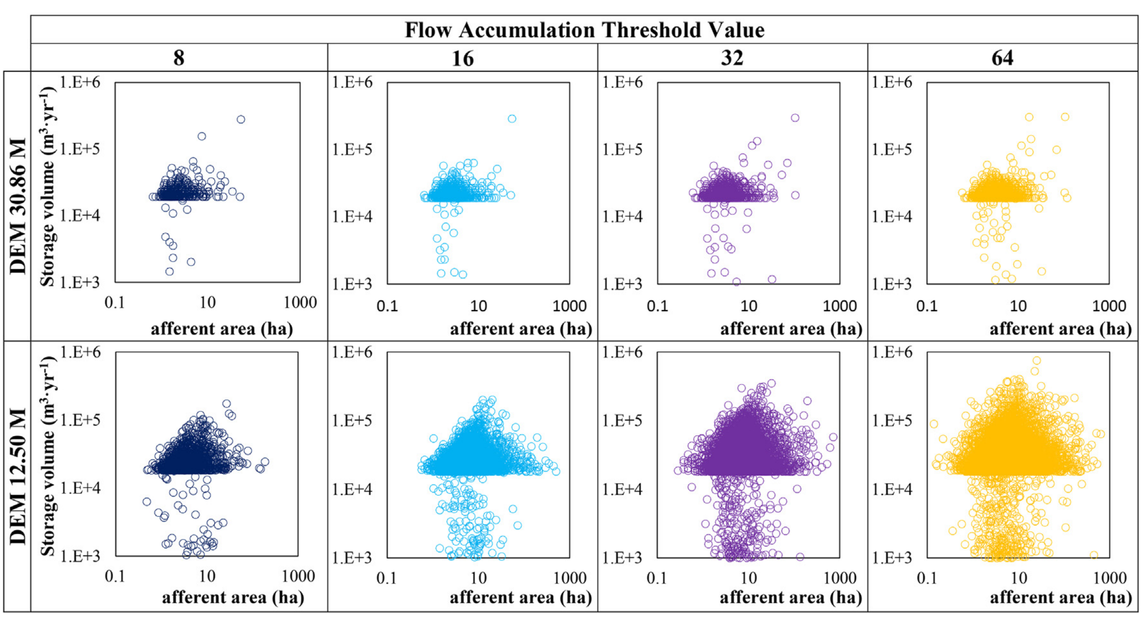

Fig. 7. Rainwater volume stored concerning the afferent area of each pond, per flow accumulation threshold value, and digital elevation model (DEM).

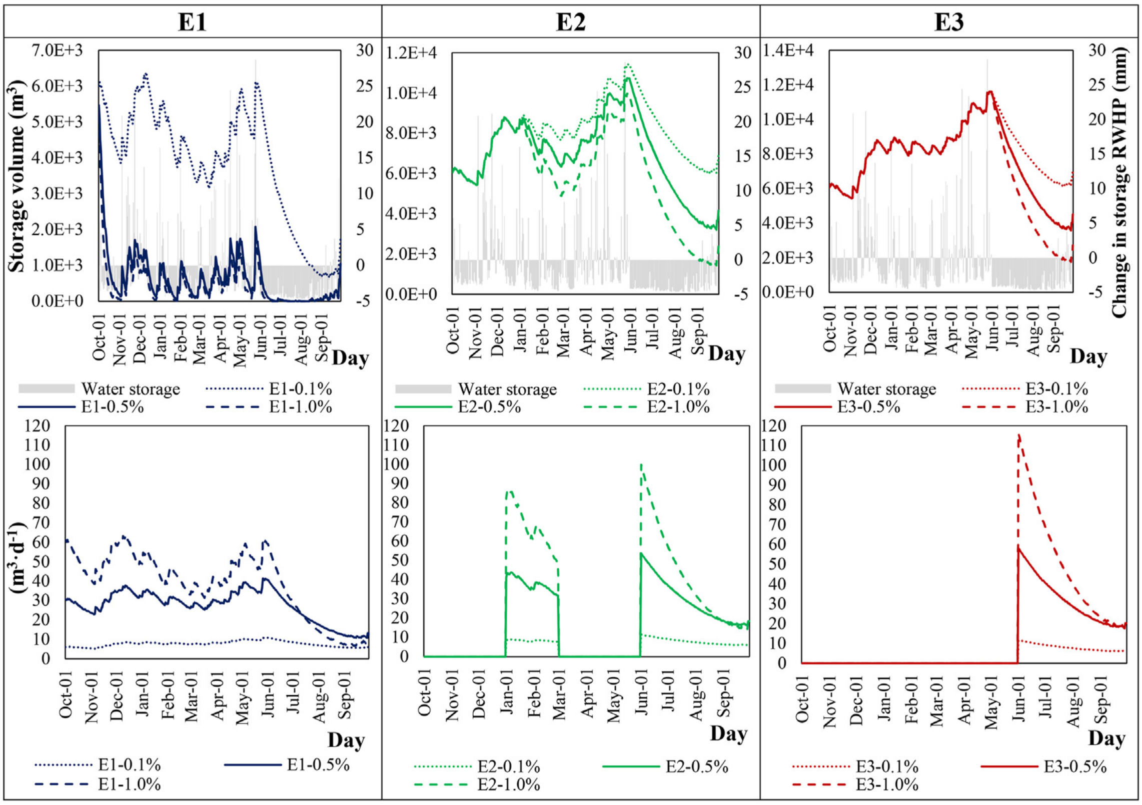

Fig. 8. Evaluation of selected ponds in three proposed simulation scenarios (E1, E2, and E3).

49.10 $m^3 \cdot day^{-1}$ for a water demand of 1.0% for the available volume in the pond.

Finally, in E3, the volume available for discharge comes from continuous storage for eight months to be used in the following four months (June, July, August, and September), where the most intense dry period is found in the study area. The average volume available for discharge in this scenario is the following: 8.02 $m^3 \cdot day^{-1}$ for a water demand of 0.1% of the available volume; 31.76 $m^3 \cdot day^{-1}$ for a water demand of 0.5%; and 48.90 $m^3 \cdot day^{-1}$ for a water demand of 1.0% of the available volume in the pond (Fig. 8).

FAO (2015) established that a water volume of 11,197 m^3 $year^{-1}$ is necessary to irrigate 1 ha of a crop all year round and that on average, one inhabitant uses 261 m^3 $year^{-1}$. In this case, it is possible to store on average 31,589 to 32,858 $m^3 \cdot day^{-1}$. Therefore, each pond, on average, could irrigate from 0.25 to 1.25 ha or supply 11 to 54 inhabitants with water every day throughout the year, according to the configuration of the water demands defined in scenarios E1, E2, and E3, which correspond to 1.0; 0.5; and 0.1% of the total volume available in the pond.

4.3. Variables that govern storage in RWHP

A dimensionality reduction was made using a principal component analysis (PCA) in the variables that influence the rainwater harvesting process, including stored volume (V_p), RWHP area (A_p), afferent area to the RWHP (A_c), precipitation ($_P$), evapotranspiration (*EVT*), change in storage in RWHP (Δ_S), slope (β), and elevation ($_E$). The analysis established two principal components (Fig. 9), PC1 and PC2, which explain 33.8% and 23.3% of the data, respectively, and together, characterize 57.1% of the sample. However, 42.9% remains unexplained, and this is because there is an influence due to the high variability of the analyzed variables that

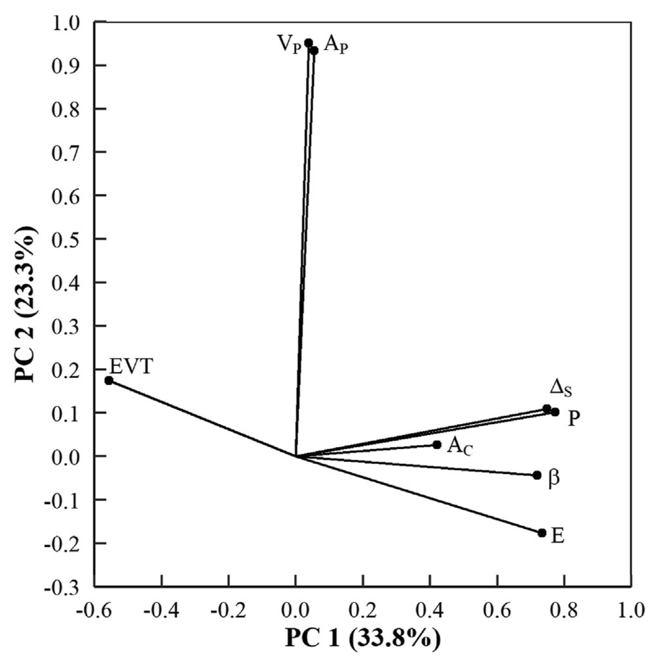

Fig. 9. Principal component analysis for the selected ponds.

were possibly not eliminated during their standardization (Khalil and Ouarda, 2009; Ouyang, 2005). Likewise, it is clear that the hydrological processes show mostly non-linear behaviors, and the PCA corresponds to a linear analysis that tries to identify the relationship between random variables.

PC1 is comprised positively by precipitation (*P*) and negatively

Table 4
Correlation coefficients between variables and principal components.

	V_p	A_p	A_c	P	EVP	n_s	β	E	PC 1	PC 2
V_p	1.00	0.84	0.03	0.06	0.06	0.08	−0.01	−0.07	0.04	0.95
A_p	0.84	1.00	0.03	0.03	0.00	0.02	0.04	−0.03	0.05	0.93
A_c	0.03	0.03	1.00	0.19	−0.13	0.18	0.29	0.21	0.42	0.03
P	0.06	0.03	0.19	1.00	−0.12	0.87	0.40	0.31	0.77	0.1
EVP	0.06	0.00	−0.13	−0.12	1.00	−0.10	−0.38	−0.61	−0.56	0.17
n_s	0.08	0.02	0.18	0.87	−0.10	1.00	0.31	0.33	0.75	0.11
β	−0.01	0.04	0.29	0.40	−0.38	0.31	1.00	0.47	0.72	−0.04
E	−0.07	−0.03	0.21	0.31	−0.61	0.33	0.47	1.00	0.73	−0.18

V_p: stored volume; A_p: rainwater harvesting pond area (RWHP); A_c: afferent area of RWHP; P: precipitation; EVP: evapotranspiration; n_s: change in storage in RWHP; β: slope; E: elevation; PC1 and PC2: principal components 1 and 2.

by evapotranspiration (*EVT*); conversely, the storage volume in RWHP (V_p) and the pond area (A_p) compose PC2 (Table 4). The correlation coefficients between the analysis variables show that the pond area (A_p) (0.84) has the highest positive correlation to obtain the volume. Similarly, variables such as evapotranspiration (*EVT*) (0.06) and afferent area (A_c) (0.03) in this study suggest a low relationship in obtaining the volume. In this sense, the stored volume tends to be independent of these variables. However, it is important to note that changes in storage at RWHP (Δ_S) is a function of precipitation and evapotranspiration; besides, the pond is a structure that facilitates the collection and storage of rainwater due to its geomorphological characteristics and its minimal interventions on the terrain. Therefore, the RWHP area (A_p) is vital as an item with storage capacity related to its size.

5. Conclusions

A new methodology focused on the detection and selection of rainwater harvesting ponds (RWHP) based on surface geomorphology was developed and implemented in the Tolima region of Colombia. From two digital elevation models with different resolutions, the curvature profile and flow accumulation values were extracted. Other physical variables such as precipitation, evapotranspiration, soil texture, and vegetation cover were necessary to calculate the water storage in RWHP and the direct runoff from the area related to RWHP. These are structures with non-convex curvature and located at some distance from current channels, covered by a waterproof coat that facilitates the storage and collection of rainwater in a particular area. The results showed that the increase in the resolution of a digital elevation model and the flow accumulation threshold value produced a significant increase in the number of RWHPs detected and selected, as well as an increase in the average volumes harvested.

The conclusion drawn from the principal component analysis is that the RWHP area is the variable with the highest impact on rainwater harvesting, i.e., the larger the pond, the higher the volume harvested.

Finally, three storage and discharge scenarios were evaluated for each of the ponds, and the results indicated that for the study area, a cycle of six months of storage and six months of discharge corresponds to the maximum volumes stored, and therefore, the highest volumes offered. This will improve the water availability of the driest period in the RWHP areas, allowing cropping to be irrigated or people to be supplied with water, or both.

Formatting of funding sources

Funding partially supported by MINCIENCIAS 812–2018 young researchers' fellowship program and the Research Office of Universidad de Ibagué [project 19-500-INT].

CRediT authorship contribution statement

Juan D. Márquez: Investigation, Formal analysis, Data curation, Validation, Writing – original draft. **Luis E. Peña:** Conceptualization, Methodology, Writing – review & editing, Supervision. **Miguel Barrios:** Conceptualization, Methodology, Writing – review & editing. **Julián Leal:** Data curation, Methodology, Visualization.

Declaration of competing interest

The authors declare that they have no known competing financial interests or personal relationships that could have appeared to influence the work reported in this paper.

Acknowledgments

Many thanks to IDEAM, IGAC, and CORTOLIMA in Colombia for providing climatological information data, the soil study of the Tolima Region, and the land cover maps of the Tolima region, respectively.

References

Adham, A., Sayl, K.N., Abed, R., Abdeladhim, M.A., Wesseling, J.G., Riksen, M., Fleskens, L., Karim, U., Ritsema, C.J., 2018. A GIS-based approach for identifying potential sites for harvesting rainwater in the Western Desert of Iraq. Int. Soil Water Conserv. Res. 6 (4), 297–304. https://doi.org/10.1016/j.iswcr.2018.07.003.
Adham, A., Wesseling, J.G., Abed, R., Riksen, M., Ouessar, M., Ritsema, C.J., 2019. Assessing the impact of climate change on rainwater harvesting in the Oum Zessar watershed in Southeastern Tunisia. Agric. Water Manag. 221, 131–140. https://doi.org/10.1016/j.agwat.2019.05.006.
Akumu, C.E., Baldwin, K., Dennis, S., 2019. GIS-based modeling of forest soil moisture regime classes: using Rinker Lake in northwestern Ontario, Canada as a case study. Geoderma 351, 25–35. https://doi.org/10.1016/j.geoderma.2019.05.014.
Ammar, A., Riksen, M., Ouessar, M., Ritsema, C., 2016. Identification of suitable sites for rainwater harvesting structures in arid and semi-arid regions: a review. Int. Soil Water Conserv. Res. 4 (2), 108–120. https://doi.org/10.1016/j.iswcr.2016.03.001.
Ariza-Villaverde, A.B., Jiménez-Hornero, F.J., Gutiérrez de Ravé, E., 2013. Multifractal analysis applied to the study of the accuracy of DEM-based stream derivation. Geomorphology 197, 85–95. https://doi.org/10.1016/j.geomorph.2013.04.040.
Ariza-Villaverde, A.B., Jiménez-Hornero, F.J., Gutiérrez de Ravé, E., 2015. Influence of DEM resolution on drainage network extraction: a multifractal analysis. Geomorphology 241, 243–254. https://doi.org/10.1016/j.geomorph.2015.03.040.
Assefa, S., Biazin, B., Muluneh, A., Yimer, F., Haileslassie, A., 2016. Rainwater harvesting for supplemental irrigation of onions in the southern dry lands of Ethiopia. Agric. Water Manag. 178, 325–334. https://doi.org/10.1016/j.agwat.2016.10.012.
Balkhair, K.S., Ur Rahman, K., 2019. Development and assessment of rainwater harvesting suitability map using analytical hierarchy process, GIS and RS techniques. Geocarto Int. 1–28. https://doi.org/10.1080/10106049.2019.1608591.
Chen, Y., Guan, Y., Shao, G., Zhang, D., 2016. Investigating trends in streamflow and precipitation in Huangfuchuan basin with wavelet analysis and the Mann-Kendall test. Water (Switzerland) 8 (3). https://doi.org/10.3390/w8030077.
Domazetović, F., Šiljeg, A., Lončar, N., Marić, I., 2019. Development of automated multicriteria GIS analysis of gully erosion susceptibility. Appl. Geogr. 112 https://

doi.org/10.1016/j.apgeog.2019.102083.
Dornik, A., Drăguţ, L., Urdea, P., 2018. Classification of soil types using geographic object-based image analysis and random forests. Pedosphere 28 (6), 913–925. https://doi.org/10.1016/S1002-0160(17)60377-1.
FAO, 2015. AQUASTAT Perfil de País - Colombia. Organización de Las Naciones Unidas Para La Alimentación y La Agricultura, Roma, Italia.
González-Álvarez, Á., Viloria-Marimón, O.M., Coronado-Hernández, Ó.E., Vélez-Pereira, A.M., Tesfagiorgis, K., Coronado-Hernández, J.R., 2019. Isohyetal maps of daily maximum rainfall for different return periods for the Colombian Caribbean Region. Water (Switzerland) 11 (2). https://doi.org/10.3390/w11020358.
Gopinath, G., Swetha, T.V., Ashitha, M.K., 2014. Automated extraction of watershed boundary and drainage network from SRTM and comparison with Survey of India toposheet. Arabian J. Geosci. 7 (7), 2625–2632. https://doi.org/10.1007/s12517-013-0919-0.
Grum, B., Hessel, R., Kessler, A., Woldearegay, K., Yazew, E., Ritsema, C., Geissen, V., 2016. A decision support approach for the selection and implementation of water harvesting techniques in arid and semi-arid regions. Agric. Water Manag. 173, 35–47. https://doi.org/10.1016/j.agwat.2016.04.018.
IGAC, 2004. Estudio general de suelos y zonificación de tierras del departamento del Tolima. In: IGAC.
Imteaz, M.A., Adeboye, O.B., Rayburg, S., Shanableh, A., 2012. Rainwater harvesting potential for southwest Nigeria using daily water balance model. Resour. Conserv. Recycl. 62, 51–55. https://doi.org/10.1016/j.resconrec.2012.02.007.
Jamali, A.A., Ghorbani Kalkhajeh, R., 2020. Spatial modeling considering valley's shape and rural satisfaction in check dams site selection and water harvesting in the watershed. Water Resour. Manag. 34 (10), 3331–3344. https://doi.org/10.1007/s11269-020-02616-2.
Jung, K., Lee, T., Choi, B.G., Hong, S., 2014. Rainwater harvesting system for continuous water supply to the regions with high seasonal rainfall variations. Water Resour. Manag. 29 (3), 961–972. https://doi.org/10.1007/s11269-014-0854-1.
Kadam, A.K., Kale, S.S., Pande, N.N., Pawar, N.J., Sankhua, R.N., 2012. Identifying potential rainwater harvesting sites of a semi-arid , basaltic region of western India , using SCS-CN method. Water Resour. Manag. 26, 2537–2554. https://doi.org/10.1007/s11269-012-0031-3.
Kanta, L., Jha, M.K., Chowdary, V.M., 2017. Multi-criteria analysis and GIS modeling for identifying prospective water harvesting and arti fi cial recharge sites for sustainable water supply. J. Clean. Prod. 142, 1436–1456. https://doi.org/10.1016/j.jclepro.2016.11.163.
Khalil, B., Ouarda, T.B.M.J., 2009. Statistical approaches used to assess and redesign surface water-quality-monitoring networks. J. Environ. Monit. 11 (11), 1915–1929. https://doi.org/10.1039/b909521g.
Kumar, S., Ramilan, T., Ramarao, C.A., Rao, C.S., Whitbread, A., 2016. Farm level rainwater harvesting across different agro climatic regions of India: assessing performance and its determinants. Agric. Water Manag. 176, 55–66. https://doi.org/10.1016/j.agwat.2016.05.013.
Kumar, T., Jhariya, D.C., 2017. Identification of rainwater harvesting sites using SCS-CN methodology, remote sensing and Geographical Information System techniques. Geocarto Int. 32 (12), 1367–1388. https://doi.org/10.1080/10106049.2016.1213772.
Li, H., Zhao, X., Gao, X., Ren, K., Wu, P., 2018. Effects of water collection and mulching combinations on water infiltration and consumption in a semiarid rainfed orchard. J. Hydrol. 558, 432–441. https://doi.org/10.1016/j.jhydrol.2018.01.052.
Luo, M., Tang, G., Dong, Y., 2008, 2008 International Workshop on Education Technology and Training and 2008 International Workshop on Geoscience and Remote Sensing, ETT and GRS. Uncertainty of Flow Accumulation Threshold Influence in Hydrology Modeling -A Case Study in Qinling Mountain SRTM3 DEM Based, vol. 2, pp. 219–222. https://doi.org/10.1109/ETTandGRS.2008.280.
MacMillan, R.A., Pettapiece, W.W., Nolan, S.C., Goddard, T.W., 2000. A generic procedure for automatically segmenting landforms into landform elements using DEMs, heuristic rules and fuzzy logic. Fuzzy Set Syst. 113 (1), 81–109. https://doi.org/10.1016/S0165-0114(99)00014-7.
Mahmoud, S.H., Alazba, A.A., 2015. The potential of in situ rainwater harvesting in arid regions: developing a methodology to identify suitable areas using GIS-based decision support system. Arabian J. Geosci. 8 (7), 5167–5179. https://doi.org/10.1007/s12517-014-1535-3.
Mbilinyi, B.P., Tumbo, S.D., Mahoo, H.F., Mkiramwinyi, F.O., 2007. GIS-based decision support system for identifying potential sites for rainwater harvesting. Phys. Chem. Earth 32 (15–18), 1074–1081. https://doi.org/10.1016/j.pce.2007.07.014.
Moore, I.D., Grayson, R.B., Ladson, A.R., 1991. Digital terrain modelling: a review of hydrological, geomorphological, and biological applications. Hydrol. Process. 5 (1), 3–30. https://doi.org/10.1002/hyp.3360050103.
Mugo, G.M., Odera, P.A., 2019. Site selection for rainwater harvesting structures in Kiambu County-Kenya. Egypt. J. Remote Sens. Space Sci. 22 (2), 155–164. https://doi.org/10.1016/j.ejrs.2018.05.003.
Napoli, M., Cecchi, S., Orlandini, S., Zanchi, C.A., 2014. Determining potential rainwater harvesting sites using a continuous runoff potential accounting procedure and GIS techniques in central Italy. Agric. Water Manag. 141, 55–65. https://doi.org/10.1016/j.agwat.2014.04.012.
National Wearher Service, 2020. Cold & Warm Episodes by Season. National Weather Service Climate Prediction Center. https://origin.cpc.ncep.noaa.gov/products/analysis_monitoring/ensostuff/ONI_v5.php.
Natural Resources Conservation Service, U. S. D. of Agriculture, 2009. Chapter 7 hydrologic soil groups. In: National Engineering Handbook, pp. 7-1–7–5. https://directives.sc.egov.usda.gov/OpenNonWebContent.aspx?content=22526.wba.
Ngigi, S.N., Savenije, H.H.G., Gichuki, F.N., 2007. Land use changes and hydrological impacts related to up-scaling of rainwater harvesting and management in upper Ewaso Ng'iro river basin, Kenya. Land Use Pol. 24 (1), 129–140. https://doi.org/10.1016/j.landusepol.2005.10.002.
Ouyang, Y., 2005. Evaluation of river water quality monitoring stations by principal component analysis. Water Res. 39 (12), 2621–2635. https://doi.org/10.1016/j.watres.2005.04.024.
Oyebande, L., Adeaga, O., 2006. Flow simulation in an ungauged basin using a digital elevation model. IAHS Publ. 309, 282–289. http://iahs.info/redbooks/a309/309033.pdf.
Peña, L.E., Barrios, M., Francés, F., 2016. Flood quantiles scaling with upper soil hydraulic properties for different land uses at catchment scale. J. Hydrol. 541, 1258–1272. https://doi.org/10.1016/j.jhydrol.2016.08.031.
Persendt, F.C., Gomez, C., 2016. Assessment of drainage network extractions in a low-relief area of the Cuvelai Basin (Namibia) from multiple sources: LiDAR, topographic maps, and digital aerial orthophotographs. Geomorphology 260, 32–50. https://doi.org/10.1016/j.geomorph.2015.06.047.
Rosell, S., Olvmo, M., Holmer, B., 2017. Cultivated land–a scarce commodity in a densely populated rural area in South Wollo, Ethiopia. J. Land Use Sci. 12 (4), 252–270. https://doi.org/10.1080/1747423X.2017.1319978.
Sayl, K.N., Muhammad, N.S., Yaseen, Z.M., El-Shafie, A., 2016. Estimation the physical variables of rainwater harvesting system using integrated GIS-based remote sensing approach. Water Resour. Manag. 30 (9), 3299–3313. https://doi.org/10.1007/s11269-016-1350-6.
Shadeed, S.M., Judeh, T.G., Almasri, M.N., 2019. Developing GIS-based water poverty and rainwater harvesting suitability maps for domestic use in the Dead Sea region (West Bank, Palestine). Hydrol. Earth Syst. Sci. 23 (3), 1581–1592. https://doi.org/10.5194/hess-23-1581-2019.
Shadmehri Toosi, A., Ghasemi Tousi, E., Ghassemi, S.A., Cheshomi, A., Alaghmand, S., 2020. A multi-criteria decision analysis approach towards efficient rainwater harvesting. J. Hydrol. 582, 124501 https://doi.org/10.1016/j.jhydrol.2019.124501.
Sharma, S.K., Tiwari, K.N., 2009. Bootstrap based artificial neural network (BANN) analysis for hierarchical prediction of monthly runoff in Upper Damodar Valley Catchment. J. Hydrol. 374 (3–4), 209–222. https://doi.org/10.1016/j.jhydrol.2009.06.003.
Singhai, A., Das, S., Kadam, A.K., Shukla, J.P., Bundela, D.S., Kalashetty, M., 2019. GIS-based multi-criteria approach for identification of rainwater harvesting zones in upper Betwa sub-basin of Madhya Pradesh, India. Environ. Dev. Sustain. 21 (2), 777–797. https://doi.org/10.1007/s10668-017-0060-4.
Terêncio, D.P.S., Sanches Fernandes, L.F., Cortes, R.M.V., Pacheco, F.A.L., 2017. Improved framework model to allocate optimal rainwater harvesting sites in small watersheds for agro-forestry uses. J. Hydrol. 550, 318–330. https://doi.org/10.1016/j.jhydrol.2017.05.003.
Tiwari, K., Goyal, R., Sarkar, A., 2018. GIS-based methodology for identification of suitable locations for rainwater harvesting structures. Water Resour. Manag. 1811–1825. https://doi.org/10.1007/s11269-018-1905-9.
Turc, L., 1961. Estimation of Irrigation water requirements, potential evapotranspiration: a simple climatic formula evolved up to date. J. Agricult. Environ. Int. Develop. 12 (1), 13–49.
USDA-SCS, 1972. Part 630 hydrology national engineering handbook chapter 10 estimation of direct runoff from storm rainfall. In: National Engineering Handbook.
Wambura, F.J., Dietrich, O., Graef, F., 2018. Analysis of infield rainwater harvesting and land use change impacts on the hydrologic cycle in the Wami River basin. Agric. Water Manag. 203, 124–137. https://doi.org/10.1016/j.agwat.2018.02.035.
Welderufael, W.A., Woyessa, Y.E., Edossa, D.C., 2013. Impact of rainwater harvesting on water resources of the modder river basin, central region of South Africa. Agric. Water Manag. 116, 218–227. https://doi.org/10.1016/j.agwat.2012.07.012.
Wu, R.S., Molina, G.L.L., Hussain, F., 2018. Optimal sites identification for rainwater harvesting in northeastern Guatemala by analytical hierarchy process. Water Resour. Manag. 32 (12), 4139–4153. https://doi.org/10.1007/s11269-018-2050-1.
Zevenbergen, L.W., Thorne, C.R., 1987. Quantitative analysis of land surface topography. Earth Surf. Process. Landforms 12 (1), 47–56. https://doi.org/10.1002/esp.3290120107.